Applied Physics Letters

Dynamic tuning of near-field radiative transport between an overlapping pair of movable comb-like metamaterials

Cite as: Appl. Phys. Lett. **118**, 153106 (2021); https://doi.org/10.1063/5.0045563
Submitted: 27 January 2021 . Accepted: 06 April 2021 . Published Online: 15 April 2021

Yang Liu, Fangqi Chen, Andrew Caratenuto, and Yi Zheng

Applied Physics Letters ARTICLE scitation.org/journal/apl

Dynamic tuning of near-field radiative transport between an overlapping pair of movable comb-like metamaterials

Cite as: Appl. Phys. Lett. **118**, 153106 (2021); doi: 10.1063/5.0045563
Submitted: 27 January 2021 · Accepted: 6 April 2021 ·
Published Online: 15 April 2021

Yang Liu, Fangqi Chen, Andrew Caratenuto, and Yi Zheng[a)]

AFFILIATIONS

Department of Mechanical and Industrial Engineering, Northeastern University, Boston, Massachusetts 02115, USA

[a)]Author to whom correspondence should be addressed: y.zheng@northeastern.edu

ABSTRACT

We present a theoretical study of nanoscale radiative thermal transport between an overlapping pair of movable comb-like SiO_2 gratings by an improved and more accurate near-field radiative heat transfer (NFRHT) method. This method does not rely on the effective medium theory (EMT) that does not take the geometric shape factors of nanostructures into account. Contrary to the EMT treating the grating structure as a homogeneous film, our improved NFRHT method can accurately predict the change of heat flux between the overlapping nanogratings for different scenarios considering surface pattern effects. The longitudinal and lateral movements of the comb-like overlapping nanogratings have been investigated to evaluate the dynamic control of NFRHT, which can be significantly modulated, resulting in heat flux ratios up to 23.5 and 5.5, respectively, for small-scale displacements. Furthermore, the NFRHT between overlapping non-contact metamaterials can exceed the intrinsic heat conduction limit for a contact mode by an order of magnitude while properly adjusting the period and relative position of the overlapping nanogratings. By taking advantage of movable metamaterials, the dynamic tuning of NFRHT and light manipulation can provide great benefit to the fields of energy harvesting and conversion, infrared sensing and detection, and thermal management technology.

When the distance between two objects in a non-equilibrium thermal system is comparable to or even less than the wavelengths of thermal radiation, the radiative heat transfer between objects primarily depends on evanescent waves.[1–5] This is especially the case when the surface polaritons are excited or when hyperbolic modes exist, which cause the near-field radiative heat flux to exceed the blackbody radiation limit by several orders of magnitude.[6–15] Due to the characteristics mentioned above, near-field radiative heat transfer (NFRHT) has a variety of applications in areas such as energy conversion technology, infrared detection technology, and thermal management.[16–31]

Many researchers have had success demonstrating the merits of NFRHT. Biehs *et al.*[32] combined the effective medium theory (EMT) and standard stochastic electrodynamics to investigate how the relative position of the optical axes of two polar/metallic misaligned gratings affects the NFRHT between the gratings at long wavelengths. Liu *et al.*[33] added a layer of graphene sheet to enhance the NFRHT between two parallel SiO_2 gratings based on the scattering-matrix approach. Besides, Liu *et al.* confirmed that, based on the scattering theory, the radiative heat flux between doped silicon gratings exceeds that between planar surfaces and can be one or even two orders of magnitude higher than what is predicted by the geometry-based Derjaguin proximity approximation.[34] Similarly, Zheng *et al.*[35] theoretically studied NFRHT between two parallel graphene-covered Si-20 gratings. Wang *et al.*[36,37] demonstrated that exciting magnetic polaritons can enhance the NFRHT between one-dimensional (1D) periodic SiC gratings and calculated the near-field radiative heat flux between two of these gratings based on the scattering matrix theory with rigorous coupled wave analysis. Although many scholars have studied the NFRHT between two parallel gratings, most of the research on tuning the NFRHT between two parallel gratings has focused on the effects of the grating material, grating filling factor, and vacuum gap between gratings on the radiative heat flux.[32,33,35–37] Furthermore, while all studies of NFRHT between gratings must consider a certain vacuum gap, the NFRHT between overlapping nanogratings has not yet been investigated prior to this work.

In this Letter, we investigate the NFRHT between an overlapping pair of movable comb-like nanogratings in the long wavelength region, which is calculated via an improved NFRHT method. This method

considers surface pattern effects so that it can predict accurately the change of heat flux between the overlapping nanogratings in different scenarios. We also study how the longitudinal and lateral movements of these comb-like overlapping nanogratings achieve the dynamic control of NFRHT. The results indicate that small-scale longitudinal and lateral movements of the nanogratings can modulate tremendously the associated NFRHT between the gratings. Furthermore, we find that by properly adjusting the period and relative position of nanogratings, the NFRHT between overlapping non-contact metamaterials exceed the intrinsic heat conduction limit for a contact mode.

The considered configuration of NFRHT between an overlapping pair of 1D movable comb-like SiO_2 nanogratings is illustrated in Fig. 1(a). In this structure, both the top and bottom geometries have 20 nm layers of SiO_2 atop 100 nm thick gold layers. A 1D SiO_2 nanograting structure of height $h = 100$ nm, grating period $\Lambda = 100$ nm, and filling ratio $\phi = w/\Lambda = 0.2$ is placed on the top of the SiO_2 film. The gold layer offers structural support for the upper SiO_2 layers and blocks radiation from reaching the substrate. The gap L represents the distance between the bottom thin film layers of the two SiO_2 nanogratings. Both of the nanogratings face each other, and one is laterally displaced with respect to the other so that the two nanogratings can overlap one another (i.e., the ridge of one nanograting faces the thin film layer of the other). The lateral displacement of two nanogratings is $a = b = 30$ nm, and their temperatures are $T_1 = 301$ K and $T_2 = 300$ K, respectively. These temperature and structural properties are used as the default case in this Letter, unless otherwise specified.

To calculate heat flux across closely spaced objects, we use the expression for NFRHT obtained through dyadic Green's function.[38] NFRHT between closely spaced objects can be calculated by[33,34,38,39]

$$Q_{1\to2}(T_1, T_2, L) = \int_0^\infty \frac{d\omega}{2\pi}[\Theta(\omega, T_1) - \Theta(\omega, T_2)]T_{1\to2}(\omega, L), \quad (1)$$

where $\Theta(\omega, T_1) = (\omega/2)\coth(\omega/2k_BT)$ is the energy of the harmonic oscillator at frequency ω and temperature T, k_B is the Boltzmann constant, and $\hbar$ is the reduced Planck constant. The function $T_{1\to2}(\omega, L)$ is the spectral transmissivity of radiative transport between media 1 and 2 separated by distance L and is given by[38,40,41]

$$T_{1\to2}(\omega, L) = \int_0^\infty \frac{k_\rho dk_\rho}{2\pi}\xi(\omega, k_\rho), \quad (2)$$

where k_ρ is the parallel component of wavevector and $\xi(\omega, k_\rho)$ is the energy transmission coefficient. The energy transmission coefficient is expressed as

$$\xi(\omega, k_\rho \le \omega/c) = \sum_{\mu=s,p} \frac{\left(1-|\tilde{R}_1^{(\mu)}|^2-|\tilde{T}_1^{(\mu)}|^2\right)\left(1-|\tilde{R}_2^{(\mu)}|^2-|\tilde{T}_2^{(\mu)}|^2\right)}{|1-\tilde{R}_1^{(\mu)}\tilde{R}_2^{(\mu)}e^{2jk_zL}|^2}, \quad (3a)$$

$$\xi(\omega, k_\rho > \omega/c) = \sum_{\mu=s,p} \frac{4\mathrm{J}\left(\tilde{R}_1^{(\mu)}\right)\mathrm{J}\left(\tilde{R}_2^{(\mu)}\right)e^{-2|k_z|L}}{|1-\tilde{R}_1^{(\mu)}\tilde{R}_2^{(\mu)}e^{-2|k_z|L}|^2}, \quad (3b)$$

where $\tilde{R}_1^{(\mu)}$ and $\tilde{R}_2^{(\mu)}$ and $\tilde{T}_1^{(\mu)}$ and $\tilde{T}_2^{(\mu)}$ are the polarized reflection and transmission coefficients of the two half spaces, $\mu = s$ (or p) refers to the transverse electric (or magnetic) polarization, and k_z is the z-component of wavevector in vacuum. The propagating and evanescent modes are represented by $k_\rho \le \omega/c$ and $k_\rho > \omega/c$, respectively. The expression can be used in multi-layered planar structures or planar media with effective dielectric properties.[18]

A schematic of the NFRHT between an overlapping pair of movable comb-like SiO_2 nanogratings is shown in Fig. 1(b). Because the relative positions of the two nanogratings overlap, the EMT is not applicable for this structure.[42–45] Therefore, this Letter introduces an improved NFRHT method which takes the geometric shape factors of nanostructures into account and employs it to calculate the NFRHT between the overlapping nanogratings. With this method, the total heat flux in a period of the nanogratings (Q_T) is divided into six heat flux components ($Q_1 \sim Q_6$), as shown in the blue dotted box in Fig. 1(b). Each heat flux component represents the heat flux between two parallel planar faces of the simulated nanostructures. The four longitudinal heat flux components (Q_1, Q_3, Q_4 and Q_5) are the near-field radiative heat fluxes between the top thin film and top grating faces of the nanogratings. The other two components (Q_2 and Q_6) are the near-field radiative heat fluxes between the sides faces of nanogratings. Due to the heat transfer between a pair of nanogratings, the

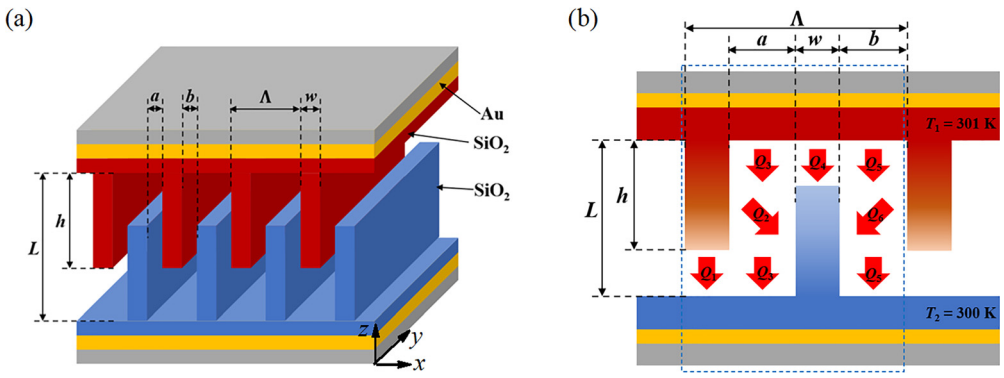

FIG. 1. (a) Schematic of an overlapping pair of movable comb-like SiO_2 nanogratings. Both sides have 1D rectangular SiO_2 nanograting as their top layers, with height $h = 100$ nm, width $w = 20$ nm, period $\Lambda = 100$ nm, and filling ratio $\phi = 0.2$. Each nanograting has a SiO_2 layer below, followed by a gold layer deposited on a substrate. The two overlapping SiO_2 nanogratings face each other with a gap L and are laterally shifted relative to one another by displacement a or b. (b) Schematic of NFRHT between an overlapping pair of movable SiO_2 nanogratings. The total heat flux (Q_T) between two SiO_2 nanogratings for a calculation period is shown in the blue dotted box, and is divided into six near-field radiative heat flux components between the opposing planes.

nanograting fins exist a temperature gradient ΔT. This work assumes that the heat conduction at the root of the grating fin is equal to the radiative heat transfer from all fin surfaces based on the energy conservation law. The expression of energy conservation for this structure is given by

$$\frac{A_1\Delta T}{R_C} = \frac{A_1(T_1 - T_2 - \Delta T)}{R_1} + \frac{A_2(T_1 - T_2 - \Delta T)X_a}{R_2} + \frac{A_6(T_1 - T_2 - \Delta T)X_b}{R_6}, \tag{4}$$

where R_C represents the heat conduction thermal resistance, and R_i represents the NFRHT thermal resistance between each plane. A_i represents the corresponding area considered in the heat transfer calculation. Here, the thermal conductivity of SiO_2 at room temperature is taken as 1.31 W m^{-1} K^{-1}. In order to investigate how the overlapped portions of the nanogratings contribute to the total heat transfer, we introduce the geometric view factors X_a and X_b to calculate the radiative heat transfer between the left and right sides of the nanogratings, respectively. These geometric view factors X_a and X_b are expressed as

$$X_a = \frac{\left(\sqrt{L^2 + a^2} + \sqrt{(2h - L)^2 + a^2}\right) - 2\left(\sqrt{(L - h)^2 + a^2}\right)}{2h}, \tag{5a}$$

$$X_b = \frac{\left(\sqrt{L^2 + b^2} + \sqrt{(2h - L)^2 + b^2}\right) - 2\left(\sqrt{(L - h)^2 + b^2}\right)}{2h}. \tag{5b}$$

Therefore, the total heat flux Q_T can be expressed as follows:

$$Q_T = \sum_{i=1}^{6} Q_i = \frac{A_1(T_1 - T_2 - \Delta T)}{R_1} + \frac{A_2(T_1 - T_2 - \Delta T)X_a}{R_2} + \frac{A_3(T_1 - T_2)}{R_3} + \frac{A_4(T_1 - T_2 - \Delta T)}{R_4} + \frac{A_5(T_1 - T_2)}{R_5} + \frac{A_6(T_1 - T_2 - \Delta T)X_b}{R_6}. \tag{6}$$

In order to explore the effect of longitudinal nanograting movement on the radiative heat transfer, we calculate the heat flux Q in a period against different gaps L using our improved NFRHT method. The calculation range of wavelength in all cases is 0.35 μm $\leq \lambda \leq$ 55 μm. To avoid the uncertainty of the applicable scope of fluctuational electrodynamics and NFRHT, the minimum longitudinal and lateral distances between the pairs of the nanograting's parallel subplans are 10 nm when a pair of nanogratings are moving. These results are displayed in Fig. 2(a). This figure illustrates that when the value of L decreases from 400 to 110 nm, the heat flux trends upwards with varying different slopes. As expected, when the value of L increases from 110 to 120 nm, a sharp decrease in the heat flux is noted. This is attributed primarily to the decrease in the heat flux components Q_1 and Q_4, because their separation distances are much less than other gaps. When L is in the range of 120 to 200 nm, the decrease in the heat flux is mainly due to the gradual decrease in the overlapping area of the nanogratings, which leads to the decrease in the heat flux Q_2 and Q_6. For the entire region I (110 nm $\leq L \leq$ 200 nm) where the two nanogratings overlap, a maximum heat flux ratio of 23.5 can be reached over a total longitudinal movement of 90 nm. In region II (200 nm $< L \leq$ 300 nm), when there is no overlap between the nanogratings, the slope of the line is larger and variable, which differs from the smaller constant slope in region III ($L >$ 300 nm). This is because the NFRHT heat flux components between the sides of nanograting (components Q_2 and Q_6) induce a greater change in region II than region III, since the side grating faces are much closer to one another in region II.

In addition, to verify the accuracy of our improved NFRHT method, we apply the EMT method to calculate NFRHT when the vacuum distance D between the two nanogratings is greater than the grating period, $D > \Lambda$.[42–46] Figure 2(b) shows the comparison of the heat fluxes Q between a pair of movable comb-like nanogratings in two scenarios of lateral displacement distribution: scenario 1, where two lateral displacements are equal ($a = b$), and scenario 2, where the two lateral displacements are different, ($a \neq b$). We calculate the heat flux for both scenarios using both the improved NFRHT method and the EMT method, setting the vacuum distance D between the nanogratings as larger than the nanograting period. Although the heat flux calculated by the improved NFRHT method is slightly larger than that calculated by the EMT method, their change trends of the heat flux with the distance are similar. The top right inset figure shows the heat flux difference ΔQ between scenarios 1 and 2, calculated by both methods. It is apparent that the heat flux difference ΔQ calculated by our improved NFRHT method decreases with an increase in vacuum distance, while the ΔQ calculated by the EMT method does not change at all in the entire distance interval. Because the EMT method does not consider the geometric shape factors of nanostructures and treats the grating structure as a homogeneous film, the lateral displacement of the nanogratings has no effect on the EMT-calculated heat flux between the nanogratings. Conversely, this improved NFRHT method considers the nanograting surface pattern effects by dividing the NFRHT between these complex nanostructures into separate NFRHT components. Each component accounts for a pair of the structure's parallel subplans, including the pairs of nanograting side faces, which allow for the accurate calculation of NFRHT when a lateral displacement is considered. Therefore, our improved NFRHT method is more reliable than the EMT method in calculating NFRHT between nanogratings.

We also calculate the spectral heat flux $dq/d\lambda$ between the two SiO_2 nanogratings with vacuum distance $D = 200$ nm and lateral displacement $a = b = 30$ nm, using both our improved NFRHT method (red curve) and the EMT method (black curve), respectively, shown in Fig. 3. It is apparent that majority of our calculated spectrum shows the same heat flux as that of the EMT method. However, our method displays two prominent peaks which are significantly greater than those of the EMT method, since our improved method considers the NFRHT between the sides of nanogratings.

To illustrate how the lateral movement of nanogratings affects the NFRHT between an overlapping pair of movable comb-like nanogratings, Fig. 4(a) shows the results for heat flux Q simulated against different lateral displacements of overlapping nanogratings. Six vacuum gaps are considered ($L = 110$, 120, 140, 160, 180, and 200 nm), and the results are calculated using the improved NFRHT method. It is apparent that the distribution of heat flux with varying lateral displacements is symmetrical, owing to the contribution of the NFRHT between the sides of the overlapping nanogratings (Q_2 and Q_6). The heat flux ratio

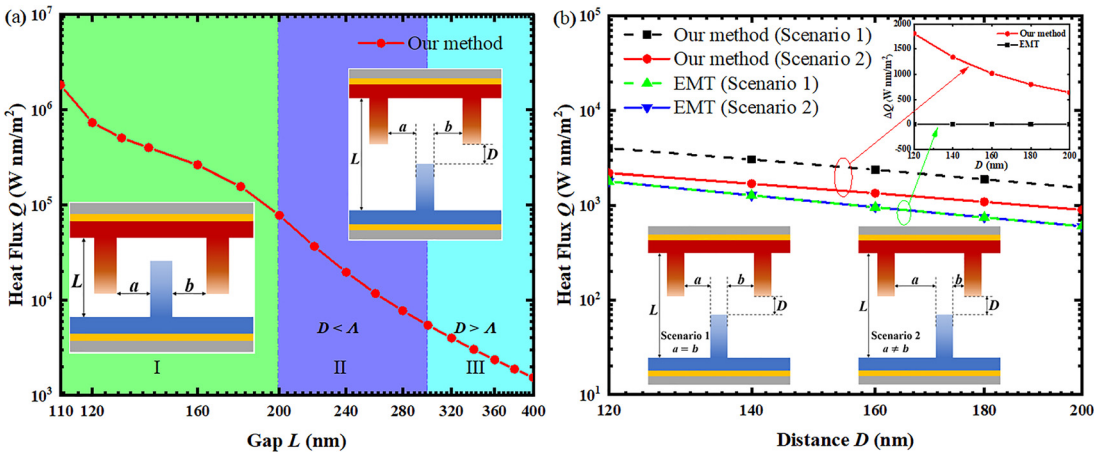

FIG. 2. (a) Radiative heat flux between a pair of movable comb-like SiO_2 nanogratings with a lateral displacement of $a = b = 30$ nm for different values of vacuum gap L. In region I ($110\text{ nm} < L \leq 200\text{ nm}$), the two nanogratings overlap. In region II ($200\text{ nm} < L \leq 300\text{ nm}$), there is no overlap, and the distance D between the nanogratings shown in the inset is less than the nanograting period. In region III ($L > 300$ nm), there is no overlap, and the distance D is larger than the nanograting period. Inset figures schematically show the associated grating overlap for the different regions. (b) Comparison of heat flux between the nanogratings in two scenarios of lateral displacement distribution. In scenario 1, the two lateral displacements are equal ($a = b$); In scenario 2, the two lateral displacements are different, ($a \neq b$). Heat fluxes in (b) are calculated by both our improved NFRHT method and the EMT method for a vacuum distance D larger than the grating period ($D > 100$ nm). Inset figures at the bottom indicate the change in the relative lateral position of a pair of movable comb-like nanogratings. The top-right inset shows heat flux differences ΔQ between scenario 1 and scenario 2 calculated by this improved NFRHT method and the EMT method.

can be as high as 5.5 for a lateral movement ($10\text{ nm} \leq a \leq 50$ nm) of the overlapping nanogratings, which proves that this lateral movement can greatly dynamically modulate the NFRHT between two overlapping nanogratings for a constant vacuum gap. In addition, the blue dotted line in Fig. 4(a) shows the heat transfer for an overlapping pair of comb-like nanogratings in contact (i.e., the gap is $L = 100$ nm and the lateral displacement is $a = b = 30$ nm). Without considering the contact thermal resistance between the nanogratings, this contact heat flux Q_c for the same calculation period is 5.24×10^8 W nm m^2. Comparing the heat flux between the contact and non-contact overlapping

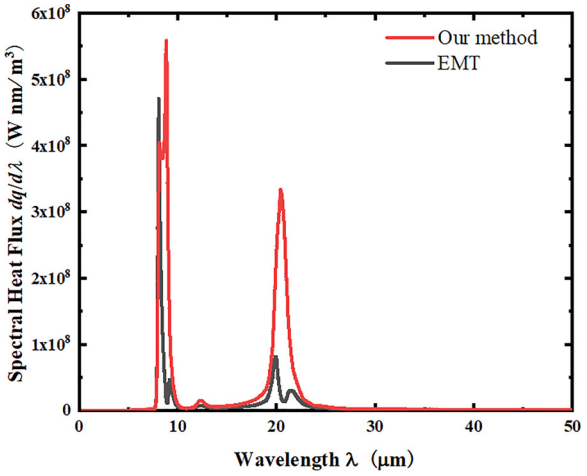

FIG. 3. Comparison of spectral heat fluxes between two SiO_2 nanogratings, with vacuum distance $D = 200$ nm and lateral displacement $a = b = 30$ nm, calculated both by our improved NFRHT method and the EMT method, respectively.

nanogratings, it can be clearly found that the heat transfer between contact nanogratings dominated by heat conduction in metamaterials is much larger than NFRHT between overlapping non-contact nanogratings for this nanostructure. Meanwhile, regardless of how a pair of nanogratings moves, the NFRHT of the non-contact case cannot exceed the heat transfer limit of the contact case.

To evaluate if the contact heat flux is larger than the NFRHT heat flux between an overlapping pair of movable comb-like nanogratings for all nanograting structures, the height of the SiO_2 nanograting is increased to $h = 1000$ nm, the nanograting lateral displacement is reduced to 10 nm (i.e., $a = b = 10$ nm), the nanograting period is decreased to 60 nm, and the nanograting width is kept the same (i.e., $w = 20$ nm and $\phi = 1/3$). Figure 4(b) shows the calculation results of the heat flux between these two movable nanogratings with various vacuum gaps L. The conduction-dominated heat transfer between contacting nanogratings (without considering the contact thermal resistance) is 5.24×10^7 W nm/m^2 shown by the blue dotted line in Fig. 4(b). Notably, when the nanograting gap L is below 1070 nm, the heat transfer between the non-contact overlapping nanogratings, which is dominated by NFRHT, is greater than that of the nanogratings in a contact mode (heat conduction limit). Furthermore, the heat transfer of the non-contact case far exceeds that of the contact case when the nanograting gap L is close to 1010 nm, contrasting with the comparison result shown in Fig. 4(a). Thus, we assert the NFRHT between overlapping non-contact metamaterials can exceed the intrinsic heat conduction limit in a contact mode by properly adjusting the period and relative position of nanogratings.

In summary, we theoretically investigate the NFRHT between an overlapping pair of movable comb-like SiO_2 nanogratings using an improved NFRHT method, which is proven to be more effective and accurate than the reported EMT method. This improved NFRHT method can accurately predict the change of heat flux between the

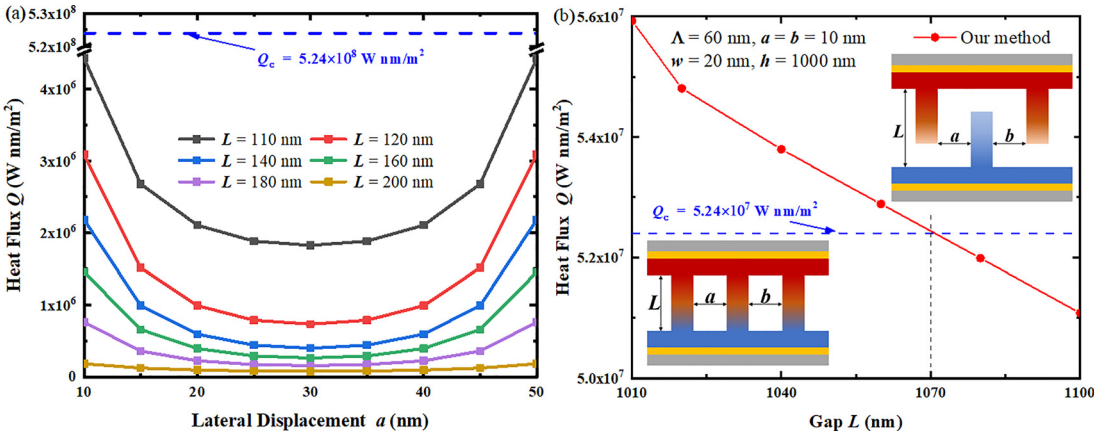

FIG. 4. (a) Radiative heat fluxes vs different lateral displacements a of an overlapping pair of movable comb-like nanogratings with six gaps ($L = 110$, 120, 140, 160, 180, and 200 nm). The heat flux Q_c represents a case where the two overlapping nanogratings contact one another, and utilizes the same calculation period as the other structures considered in (a). (b) Radiative heat fluxes vs different gaps L between two overlapping nanogratings with a lateral displacement $a = b = 10$ nm, the nanograting period $\Lambda = 60$ nm, the nanograting height $h = 1000$ nm, and the nanograting width $w = 20$ nm (i.e., the filling ratio $\phi = 1/3$). The contact heat flux Q_c for the geometry in (b) is also included.

overlapping nanogratings in different scenarios because it considers the surface pattern effects of nanogratings. This study shows that the longitudinal and lateral movements of the comb-like overlapping nanogratings can modulate tremendously the NFRHT between overlapping nanogratings, resulting in the heat flux ratios up to 23.5 and 5.5, respectively, using a small-scale displacement. Additionally, it has been demonstrated that the NFRHT between overlapping non-contact metamaterials can exceed the intrinsic heat conduction limit in a contact mode when the period and the relative position of the overlapping nanogratings are properly adjusted. It verifies the possibility of improving NFRHT utilizing relative overlapping position of movable nanostructures. This work will shed light on various promising applications in dynamic tuning of nanoscale thermal transport.

This work was supported by the National Science Foundation (No. CBET-1941743).

DATA AVAILABILITY

The data that support the findings of this study are available from the corresponding author upon reasonable request.

REFERENCES

[1]D. Polder and M. V. Hove, Phys. Rev. B **4**, 3303 (1971).
[2]A. I. Volokitin and B. N. J. Persson, Rev. Mod. Phys. **79**, 1291 (2007).
[3]A. Narayanaswamy and G. Chen, Appl. Phys. Lett. **82**, 3544 (2003).
[4]J. B. Pendry, J. Phys. **11**, 6621 (1999).
[5]J. L. Song, Q. Cheng, B. Zhang, L. Lu, and R. Hu, Rep. Prog. Phys. **84**, 036501 (2021).
[6]M. Francoeur, M. P. Mengü, and R. Vaillon, J. Quant. Spectrosc. Radiat. Transfer **110**, 2002 (2009).
[7]T. Kralik, P. Hanzelka, M. Zobac, V. Musilova, T. Fort, and M. Horak, Phys. Rev. Lett. **109**, 224302 (2012).
[8]S. Shen, A. Narayanaswamy, and G. Chen, Nano Lett. **9**, 2909 (2009).
[9]S. Basu, Z. M. Zhang, and C. J. Fu, Int. J. Energy Res. **33**, 1203 (2009).
[10]Y. M. Xuan, Photonics Nanostruct. **12**, 93 (2014).
[11]R. S. Ottens, V. Quetschke, S. Wise, A. A. Alemi, R. Lundock, G. Mueller, D. H. Reitze, D. B. Tanner, and B. F. Whiting, Phys. Rev. Lett. **107**, 014301 (2011).
[12]B. Song, D. Thompson, A. Fiorino, Y. Ganjeh, P. Reddy, and E. Meyhofer, Nat. Nanotechnol. **11**, 509 (2016).
[13]A. Fiorino, D. Thompson, L. Zhu, B. Song, P. Reddy, and E. Meyhofer, Nano Lett. **18**, 3711 (2018).
[14]M. Lim, J. Song, S. Lee, and B. Jae, Nat. Commun. **9**, 4302 (2018).
[15]J. DeSutter, L. Tang, and M. Francoeur, Nat. Nanotechnol. **14**, 751 (2019).
[16]F. Q. Chen *et al.*, Adv. Eng. Mater. **23**(2), 2000825 (2021).
[17]A. Ghanekar, J. Ji, and Y. Zheng, Appl. Phys. Lett. **109**, 123106 (2016).
[18]A. Ghanekar, M. Ricci, Y. P. Tian, O. Gregory, and Y. Zheng, Appl. Phys. Lett. **112**, 241104 (2018).
[19]J. l Song, L. Lu, B. W. Li, B. Zhang, R. Hu, X. P. Zhou, and Q. Cheng, Int. J. Heat Mass Transfer **150**, 119346 (2020).
[20]K. Joulain, J. Drevillon, and P. Ben-Abdallah, Phys. Rev. B **81**, 165119 (2010).
[21]M. Francoeur, S. Basu, and S. J. Petersen, Opt. Express **19**, 18774 (2011).
[22]K. Park, S. Basu, W. P. King, and Z. M. Zhang, J. Quant. Spectrosc. Radiat. Transfer **109**, 305 (2008).
[23]J. L. Song and Q. Cheng, Phys. Rev. B **94**, 125419 (2016).
[24]Z. Wang, P. Lv, M. Becton, J. Hong, L. Zhang, and X. Chen, Langmuir **36**, 12038 (2020).
[25]J. L. Song, Q. Cheng, L. Lu, B. W. Li, and X. P. Zhou, Phys. Rev. Appl. **13**, 024054 (2020).
[26]Y. H. Kan, C. Y. Zhao, and Z. M. Zhang, Phys. Rev. Appl. **13**, 014069 (2020).
[27]L. Tang, J. Desutter, and M. Francoeur, ACS Photonics **7**, 1304 (2020).
[28]M. Lim, J. Song, S. S. Lee, J. Lee, and B. J. Lee, Phys. Rev. Appl. **14**, 014070 (2020).
[29]G. F. Ju, T. B. Wang, D. J. Zhang, W. X. Liu, and Q. H. Liao, J. Quant. Spectrosc. Radiat. Transfer **263**, 107543 (2021).
[30]C. Zhou, Q. Lei, Y. Zhang, and H. L. Yi, Phys. Rev. B **102**, 245421 (2020).
[31]A. Fiorino, D. Thompson, L. Zhu, R. Mittapally, S. A. Biehs, O. Bezencenet, N. El-Bondry, S. Bansropun, P. Ben-Abdallah, and E. Meyhofer, ACS Nano **12**, 5774 (2018).
[32]S. A. Biehs, F. S. S. Rosa, and P. Ben-Abdallah, Appl. Phys. Lett. **98**, 243102 (2011).
[33]X. L. Liu and Z. M. Zhang, Appl. Phys. Lett. **104**, 251911 (2014).
[34]X. L. Liu, B. Zhao, and Z. M. Zhang, Phys. Rev. A **91**, 062510 (2015).
[35]Z. Zheng, A. Wang, and Y. Xuan, J. Quant. Spectrosc. Radiat. Transfer **208**, 86 (2018).
[36]Y. Yang and L. Wang, Phys. Rev. Lett. **117**, 044301 (2016).
[37]Y. Yang, P. Sabbaghi, and L. Wang, Int. J. Heat Mass Transfer **108**, 851 (2017).

[38]A. Narayanaswamy and Y. Zheng, J. Quant. Spectrosc. Radiat. Transfer **132**, 12 (2014).
[39]J. Lussange, R. Guérout, F. S. S. Rosa, J. J. Greffet, A. Lambrecht, and S. Reynaud, Phys. Rev. B **86**, 085432 (2012).
[40]Y. Yang, S. Basu, and L. Wang, J. Quant. Spectrosc. Radiat. Transfer **158**, 69 (2015).
[41]A. Ghanekar, L. Lin, J. Su, H. Sun, and Y. Zheng, Opt. Express **23**, A1129 (2015).
[42]D. H. Raguin and G. M. Morris, Appl. Opt. **32**, 1154 (1993).
[43]P. Lalanne and D. Lemercier-Lalanne, J. Mod. Opt. **43**, 2063 (1996).
[44]Y. B. Chen, Z. M. Zhang, and P. J. Timans, J. Heat Transfer **129**, 79 (2007).
[45]E. N. Glytsis and T. K. Gaylord, Appl. Opt. **31**, 4459 (1992).
[46]X. L. Liu, T. J. Bright, and Z. M. Zhang, J. Heat Transfer **136**, 092703 (2014).